

Analysis of phase-locked oscillations in multi-channel single-unit spike activity with wavelet cross-spectrum

Daeyeol Lee *

Department of Brain and Cognitive Sciences, Center for Visual Science, University of Rochester, Rochester, NY 14627, USA

Received 30 August 2001; received in revised form 18 December 2001; accepted 20 December 2001

Abstract

Electrophysiological measures of neural activity frequently display oscillatory patterns at various frequencies. Furthermore, these oscillatory patterns can become dynamically synchronized across a wide region of the brain in a task-dependent manner. In this study, phase-locked oscillations in simultaneously recorded spike trains were analyzed using the wavelet cross-spectrum. Adaptation of the existent methods of calculating wavelet cross-spectrum to spike train data was straightforward. In contrast, new methods were needed for evaluating the statistical significance of the cross-spectrum. Although a permutation test based on a large number of re-sampled cross-spectra can provide a reliable estimate of statistical significance, this was quite time-consuming. As an alternative, statistical significance was determined with a normal probability density function estimated from a small number of re-sampled cross-spectra. When applied to neuron pairs recorded in the primate supplementary motor area, the re-sampling procedure produced a reliable outcome even when it was based on as few as ten re-sampled cross-spectra. These results suggest that the wavelet analysis in combination with a re-sampling procedure provides a useful tool to examine the dynamic patterns of temporal correlation in cortical spike trains. © 2002 Elsevier Science B.V. All rights reserved.

Keywords: Cross-spectrum; Permutation test; Spike synchrony; Wavelet transform

1. Introduction

In studying complex systems, such as the brain, the efficiency of investigation is often limited by the spatial and temporal scales of the methods used to collect and analyze the data. In the analysis of extracellularly recorded single-unit activity (i.e. spike trains), the most common approach has been to analyze the number of spikes during subjectively defined temporal epochs that are linked to various sensory and motor events, such as the onset of sensory stimulus or motor response. Typically, these temporal epochs are a few hundred milliseconds long. Although these methods are arbitrary, they are often justified by the assumption that information processed by individual neurons is represented in the slowly varying rate of spikes (see Shadlen and Movshon, 1999).

There is, however, an accumulating body of evidence suggesting that different groups of neurons may be dynamically linked together by spikes synchronized on a millisecond scale (see Gray, 1999; Singer, 1999). Furthermore, numerous studies have indicated that such synchronized neural activity is often accompanied by oscillatory rhythms of various frequencies. In some cases, this was indirectly demonstrated by examining the scalp EEG recordings in human subjects performing various cognitive tasks (Csibra et al., 2000; Gevins et al., 1997; Sarnthein et al., 1998; Mima et al., 2001; Miltner et al., 1999; Rodriguez et al., 1999; Tallon-Baudry et al., 1997, 1998; Srinivasan et al., 1999; Tononi et al., 1998; von Stein et al., 1999). In other cases, the recordings of local field potentials or multi-channel single-unit activity provided more direct evidence (Baker et al., 2001; Bressler et al., 1993; Eckhorn et al., 1988; Fries et al., 1997, 2001; Gail et al., 2000; Gray and Singer, 1989; Sanes and Donoghue, 1993; Roelfsema et al., 1997; von Stein et al., 2000).

Regardless of the physical methods used to record neural activity from the brain, analytical methods are

* Tel.: +1-716-275-8677; fax: +1-716-271-3043.
E-mail address: dlee@cvs.rochester.edu (D. Lee).

required to visualize potential synchronization or consistent phase relationship in multiple oscillatory signals and to evaluate their statistical significance. Traditionally, methods based on Fourier transforms, such as Fourier power spectrum, have been applied to characterize oscillatory patterns in neural activity. The utility of such methods is intrinsically limited, however, to stationary processes in which the statistical properties of the signals can be assumed to remain invariant over time. These problems can be partially overcome by performing a series of Fourier transforms with a sliding window (sliding or short-time Fourier transform, Gail et al., 2000; Portnoff, 1980). Alternatively, methods based on wavelet transforms can be applied. Wavelet transforms have advantages over the Fourier transforms because they can be optimized in both time and frequency domains (Percival and Walden, 2000; Torrence and Compo, 1998). The wavelet transforms have been previously applied to the analysis of EEG data (Csibra et al., 2000; Isoglu-Alkaç et al., 2000; Le Van Quyen et al., 2001; Sakowitz et al., 2001; Tallon-Baudry et al., 1997, 1998). The present report demonstrates that the cross-spectrum computed from the wavelet transforms of simultaneously recorded spike trains can reveal phase-locked oscillation between them. New methods to evaluate the statistical significance of such wavelet cross-spectrum are also described.

2. Methods

2.1. Animal preparation and data collection

Multi-channel single-unit activity was recorded from the supplementary motor area of a rhesus monkey using an Eckhorn 16-channel microelectrode manipulator (Thomas Recording, Giessen, Germany) and a Plexon multi-channel acquisition processor (Plexon Inc., Dallas, TX). The arrival times of spikes were originally stored with a 25 μ s resolution and later binned with a 1 ms resolution. The animal, which was seated in a custom-built primate chair with its head fixed, produced a series of visually-guided reaching movements with its right hand on a touch screen. The touch screen was installed horizontally in front of the animal, and therefore did not block the view of the computer screen on which visual stimuli were presented. The position of the animal's hand on the touch screen was indicated to the animal as a feedback cursor on the computer screen. Targets were presented in a 4 \times 4 grid on a computer screen, and the animal was required to acquire ten successive targets in a given trial to receive a drop of apple juice. The interval between the acquisition of a given target and the presentation of the next target (response–stimulus-interval, RSI) was always 250 ms.

These experiments were performed as part of a project to study the effects of practice on neural activity, and therefore, target locations were randomized only in a small number of trials (once in a block of eight trials). For the remaining trials, the following three patterns, generated from a set of five targets (A–E) that were randomly selected for each recording session, were repeatedly presented: ABCABCABCA (5/8 trials), DECDECDECD (1/8 trials), and DECDECABC (1/8 trials).

In most neurophysiological studies, a particular event, such as the onset of sensory stimulus, occurs once in each trial. The data presented in this report were, however, obtained from an experiment in which the animal produced a series of movements in response to multiple target presentations in a given trial. Therefore, to avoid confusion, the temporal epoch surrounding the onset of a single target and the corresponding movement is referred to as an *observation window*. In the present analysis, the observation window included a 1000 ms interval starting from 400 ms before target onset.

2.2. Time-resolved cross-correlation function (*TrCCF*)

Synchronized oscillation of neural activity has often been described by the cross-correlation function (CCF). Denoting the spike train from a neuron j as:

$$x_j^n(t) = \begin{cases} 1, & \text{if there is a spike between } t \text{ and } t + \Delta t \\ 0, & \text{otherwise} \end{cases}$$

where t indicates time from target onset, n is the index for multiple observation windows ($n = 1, 2, \dots, N$) and $\Delta t = 1$ ms, the CCF between the neurons j and k can be defined as:

$$\text{CCF}_{jk}(\tau) = \frac{1}{N} \sum_n \sum_t x_j^n(t) x_k^n(t + \tau)$$

where T ($= 1000$ ms) denotes the duration of the observation window.

Periodic modulations in the CCF indicate a consistent phase relationship in the oscillatory activity of the two neurons. For example, a peak at the zero lag in the CCF indicates that the two neurons display a tendency to fire synchronously. For stationary processes, the CCF adequately describes the nature of statistical dependencies between them. Spike trains are not stationary, however, when they are influenced by external events. In such cases, the joint peri-event time histogram (JPTH) has been commonly applied (Aertsen et al., 1989). The JPTH can be defined as:

$$\text{JPTH}_{jk}(t_1, t_2) = \frac{1}{N} \sum_n x_j^n(t_1) x_k^n(t_2)$$

where t_1 and t_2 denote time from target onset. For a pair of neurons with synchronized spike activity, the JPTH

increases its value along a diagonal line (i.e. $t_1 = t_2$). For visualization of synchronization of relatively high frequency oscillation, however, it is more convenient to adopt two different time scales, one for the timing of spikes in one neuron and the other for the time lag for pairs of spikes from the two neurons (Baker et al., 2001). For example, the TrCCF can be defined as:

$$\text{TrCCF}_{jk}(t, \tau) = \text{JPTH}_{jk}(t, t + \tau) = \frac{1}{N} \sum_n x_j^n(t) x_k^n(t + \tau)$$

where t denotes time from target onset, and τ is the time lag. For graphical illustration, the raw TrCCF was smoothed with a 2-dimensional Gaussian kernel. Different widths of the Gaussian kernel ($\sigma_x = 40$ and $\sigma_y = 4$ ms) were used for the horizontal (time relative to target onset) and vertical (time lag) directions, since these two axes represent different features.

2.3. Wavelet cross-spectrum

The wavelet transform of a spike train from neuron j in the n -th observation window can be defined as:

$$W_j^n(t, s) = s^{-1/2} \sum_{\tau} x_j^n(\tau) \psi^* \left[\frac{(\tau - t)}{s} \right]$$

where $\psi[\]$ denotes a wavelet function, and the symbol (*) the complex conjugate (Torrence and Compo, 1998). The variables t and s indicate the time and scale of the wavelet function. Thus, the wavelet transform is calculated by convolving the spike train with wavelet functions with various scales (Fig. 1). The wavelet function must have a zero mean and be localized in both time and frequency space (referred to as admissibility condition). The Morlet function satisfies such requirements, and is defined as:

$$\psi(\eta) = \pi^{-1/4} e^{i\omega_0\eta} e^{-\eta^2/2}$$

where η is the non-dimensional time parameter, and ω_0 is taken to be 6 to satisfy the admissibility conditions for the wavelet function. Morlet wavelet function includes both real and imaginary parts, and this allows one to identify the amplitude and phase of different frequency

components simultaneously. In addition, the Fourier frequency for the Morlet wavelet function is approximately the inverse of the scale parameter (Meyers et al., 1993).

The wavelet cross-spectrum for the two spike trains from neurons j and k in the n -th observation window can be defined as $W_j^n(t, s)W_k^{n*}(t, s)$. In the present study, the main question concerns whether the oscillatory activity in a pair of neurons display a consistent phase relationship across multiple trials. To address this issue, the average wavelet cross-spectrum for the neurons j and k , $\text{AWCS}_{jk}(t, s)$, was calculated as:

$$\text{AWCS}_{jk}(t, s) = \frac{1}{N} \sum_n W_j^n(t, s) W_k^{n*}(t, s)$$

The average wavelet cross-spectrum as well as its single-trial version consists of complex numbers, and its amplitude (power) and phase can be defined as its absolute value and angle, respectively. It should be noted that the amplitudes of the average wavelet cross-spectrum would be relatively small if there is no consistent phase relationship between a pair of neurons. This is because cross-spectra with opposite phases get cancelled out through summation in the complex plane.

2.4. Evaluation of statistical significance

2.4.1. Shift predictor

Temporally correlated neural activity can originate from at least two different sources. On the one hand, correlated activity might be produced when a pair of neurons is activated together by a series of external events (either sensory stimuli or motor outputs), and this can be referred to as exogenous correlation. On the other hand, correlated activity might arise independently of such external factors, as a part of the dynamical processes representing various types of information in the brain, and this can be referred to as endogenous correlation. For the CCF, a traditional approach to dissociate these two different types of temporal correlation has been to apply the shift predictor (Perkel et al., 1967). In this method, a surrogate CCF is computed through a re-sampling procedure, in which the spike train from one neuron in a given trial is randomly paired with that from the second neuron in another trial in the same experimental condition. Since this procedure would preserve the exogenous temporal correlation, the difference between this re-sampled CCF and the original CCF reflects the amount of endogenous correlation. The shift predictor method can be adapted to evaluate the statistical significance of the TrCCF and the wavelet cross-spectrum (see below).

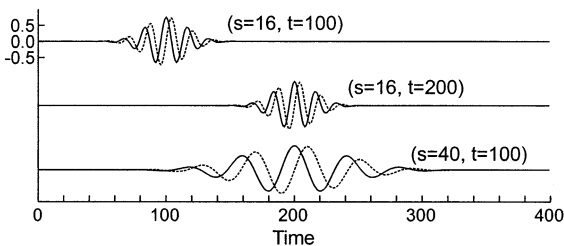


Fig. 1. Examples of Morlet wavelet functions illustrated for two different scales ($s = 16$ and 40) and two different times ($t = 100$ and 200). Morlet wave functions are complex, and thus have real (continuous lines) and imaginary (dotted lines) components.

2.4.2. Estimating TrCCF from spike density functions

In the case of the TrCCF, one can obtain the theoretical TrCCF expected for a pair of neurons without any functional interaction, using a different method than the shift predictor (Baker et al., 2001). First, the firing rates of individual neurons are estimated for each trial, and this can be achieved by using any of a large number of methods available (Pauluis and Baker, 2000). In the present study, the firing probability of individual neurons in a given observation window is calculated by the use of Gaussian kernel ($\sigma = 25$ ms; MacPherson and Aldridge, 1979). Next, assuming that the two spike trains are statistically independent, the TrCCF for a given trial can be estimated by the product of these spike density functions (SDF). Denoting the spike density function for neuron j in trial n as $F_j^n(t)$, the TrCCF estimated for independent spike trains was obtained as the following.

$$\text{TrCCF}_{jk}^{\text{est}}(t, \tau) = \frac{1}{N} \sum_n F_j^n(t) F_k^n(t + \tau)$$

This is different from a more common approach in which the SDFs are estimated from the activity averaged across a large number of observation windows (trials). However, the use of the trial-averaged SDFs might be misleading, because cortical neurons often display correlated changes in their activity across multiple trials (Baker et al., 2001; Gawne and Richmond, 1993; Lee et al., 1998; Zohary et al., 1994). Estimating the TrCCF based on the trial-averaged SDFs, therefore, would lead to the underestimation of the expected correlation in the TrCCF.

2.4.3. Statistical significance of the wavelet cross-spectrum

In principle, it might be possible to determine the statistical significance of wavelet cross-spectrum by deriving its probability density function analytically. In practice, this would be difficult, because one would first have to obtain accurate parametric models of spike trains for individual neurons, and then follow the evolution of various probability density functions through the multiple steps involved in calculating the wavelet cross-spectrum. Another approach would be to estimate empirically the associated probability density functions based on a re-sampling procedure. For example, one can generate a large number of re-sampled wavelet cross-spectra, and the P -value can be computed for each time and frequency combination by counting the number of re-sampled cross-spectra in which the amplitude of the re-sampled cross-spectra exceeds that of the original cross-spectrum, and dividing it by the number of re-sampled cross-spectra. However, there were several problems in applying this method to the current situation. First, the wavelet cross-spectrum in

the present analysis was calculated from the average of several thousand movements, and therefore calculating each re-sampled cross-spectrum was a computer-intensive and time-consuming process, taking ~ 5 min/re-sample on an 800 MHz pentium III personal computer. Second, the reliability of estimated P values increases with the number of re-sampled cross-spectra. To obtain P values with 0.001 accuracy, for example, one would require at least 10 000 re-samples, and therefore it would take ~ 1 month [$10\,000 \times 5$ (min) / $\{60$ (min/h) $\times 24$ (h per days)} = 34.7 days] to analyze a pair of neurons.

Alternatively, one can approximate the probability density function for the amplitude of average wavelet cross-spectrum with a theoretical (e.g. normal) probability density function. Although the frequency histogram for the amplitude of average cross-spectrum often displayed a substantial skew, application of square-root transformation normalized the distribution of the amplitude in most cases (see Section 3). Therefore, the probability density function of a wavelet cross-spectrum was approximated by a normal distribution based on the mean and the standard deviation (S.D.) calculated from a small number ($n = 10$) of cross-spectra after square root transformation. The normal probability distribution function $f(x)$ with a mean μ and a S.D. σ is defined as:

$$f(x) = \frac{1}{\sigma\sqrt{2\pi}} \exp\left(-\frac{(x - \mu)^2}{2\sigma^2}\right)$$

Once the probability density function is estimated, the P -value for the observed amplitude of the cross-spectrum can be obtained by calculating the area under the probability density function beyond the value corresponding to the observed amplitude. Whether the distribution of re-sampled cross-spectra followed normal distributions after square root transformation was checked by a series of Kolmogorov–Smirnov goodness-of-fit tests performed separately for each time and frequency combination. These tests were performed using a group of 200 re-sampled wavelet cross-spectra.

3. Results

The TrCCF for a pair of neurons recorded simultaneously from the supplementary motor area is shown in Fig. 2. Several alternating horizontal bands of light and dark regions lasting for about 150 ms before target onset are visible in both the raw and the smoothed TrCCF (Fig. 2A and D), suggesting that these two neurons displayed a certain degree of phase-locked oscillation. To identify the level of such phase-locked oscillation independently from the pattern expected for correlated modulation arising from exogenous factors, the TrCCF estimated from the two neurons' SDF was also calcu-

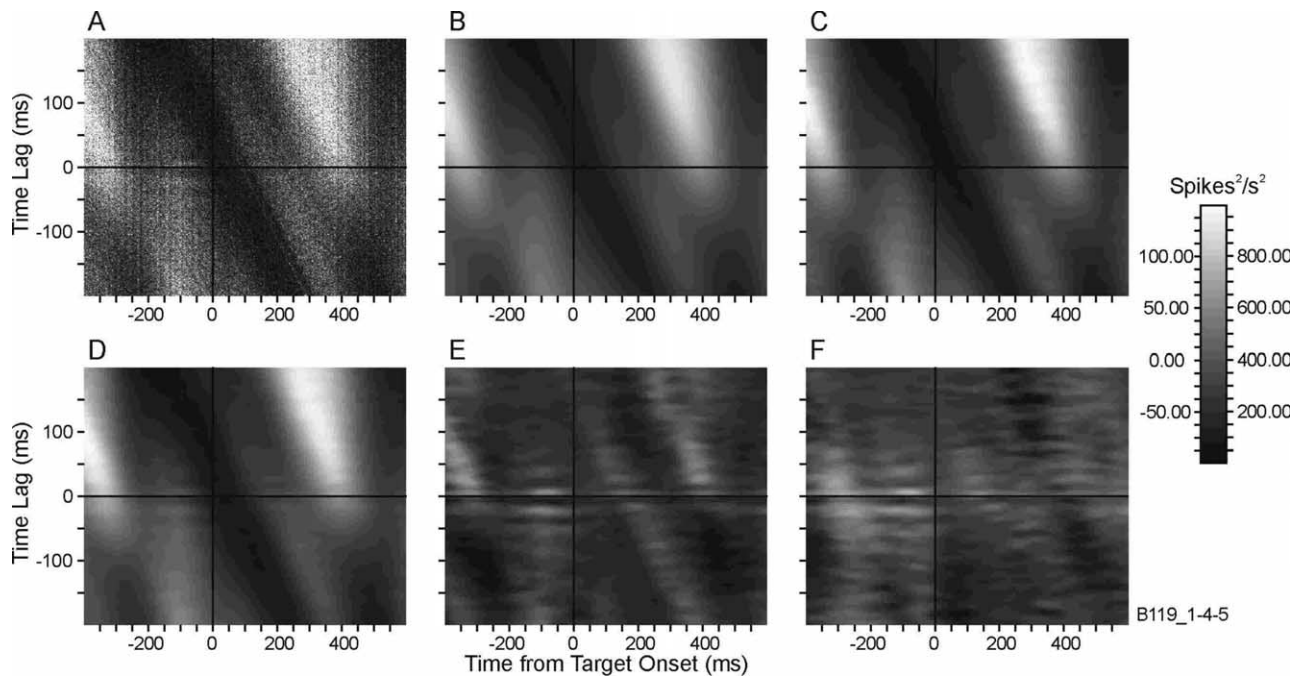


Fig. 2. TrCCF for a pair of neurons recorded simultaneously from the supplementary motor area of a monkey performing a reaching task. A. Raw TrCCF. B. Expected TrCCF based on trial-by-trial estimates of individual neuron's SDF. C. TrCCF calculated using the shift predictor method. D. Smoothed TrCCF. This was computed by convolving the raw TrCCF with a 2-dimensional (2-D) Gaussian filter ($\sigma_x = 40$ ms, $\sigma_y = 4$ ms). E. Smoothed TrCCF after subtracting the expected TrCCF (B). F. Smoothed TrCCF after subtracting the shift predictor TrCCF (C). The values on the right side of the scale bar apply to A–D, and those on the left to E and F.

lated (Fig. 2B). In addition, the shift predictor method was used to generate another estimate of the TrCCF expected for the two independent spike trains (Fig. 2C). The results from these two different methods were similar. Consequently, the subtraction of these expected TrCCF from the original ones also produced similar results, and in both cases, a series of horizontal bands suggest robust, endogenous phase-locked oscillation between these two neurons (Fig. 2E and F).

Although TrCCFs are useful in visualization of phase-locked oscillation in spike trains, they are not optimal for precise measurement of phase-locked oscillation as a function of time, and this is the main motivation for introducing methods based on the wavelet transform. For the same pair of neurons shown in Fig. 2, the amplitude and phase of the wavelet cross-spectrum is displayed in Fig. 3. Compared with the amplitude of the cross-spectrum calculated for the shift predictor (Fig. 3B), the amplitude plot for the original cross-spectrum (Fig. 3A) displayed a strong peak at 35 Hz, which is in the frequency range referred to as the γ -band in the EEG literature. At this frequency, the amplitude reached its peak approximately 85 ms prior to the target onset. In addition to this peak, the amplitude of the original cross-spectrum was often higher in many other frequency and time combinations, compared with that of the shift predictor, suggesting that even relatively

weak oscillatory activity of these two neurons tended to maintain a consistent phase relationship over a broad range of frequency throughout the observation window used in this analysis. Another advantage of the wavelet transform is that it provides an accurate estimate of phase relationship (Fig. 3C). For the frequency of 35 Hz, which included the maximum amplitude, the phase is plotted separately for closer examination (Fig. 4). At 85 ms prior to target onset, when the cross-spectrum reached its peak value at 35 Hz, its phase was -62° , corresponding to a time lag of approximately 5 ms for this frequency. Although phase values varied substantially throughout the window of analysis, the value of approximately -62° remained stable for about 150 ms, which is approximately the duration of the peak in the cross-spectrum. Therefore, for this pair of neurons, oscillatory activity was phase-locked, but it was not completely synchronized.

To evaluate the statistical significance of various peaks in the wavelet cross-spectrum, two different methods were compared. Each of these methods assigned P -values to all possible time and frequency combinations for the amplitude in the wavelet cross-spectrum. First, a permutation test was used to derive P -values from a series of empirical probability density functions based on 200 re-sampled wavelet cross-spectra. Although this permutation test does not rely on any

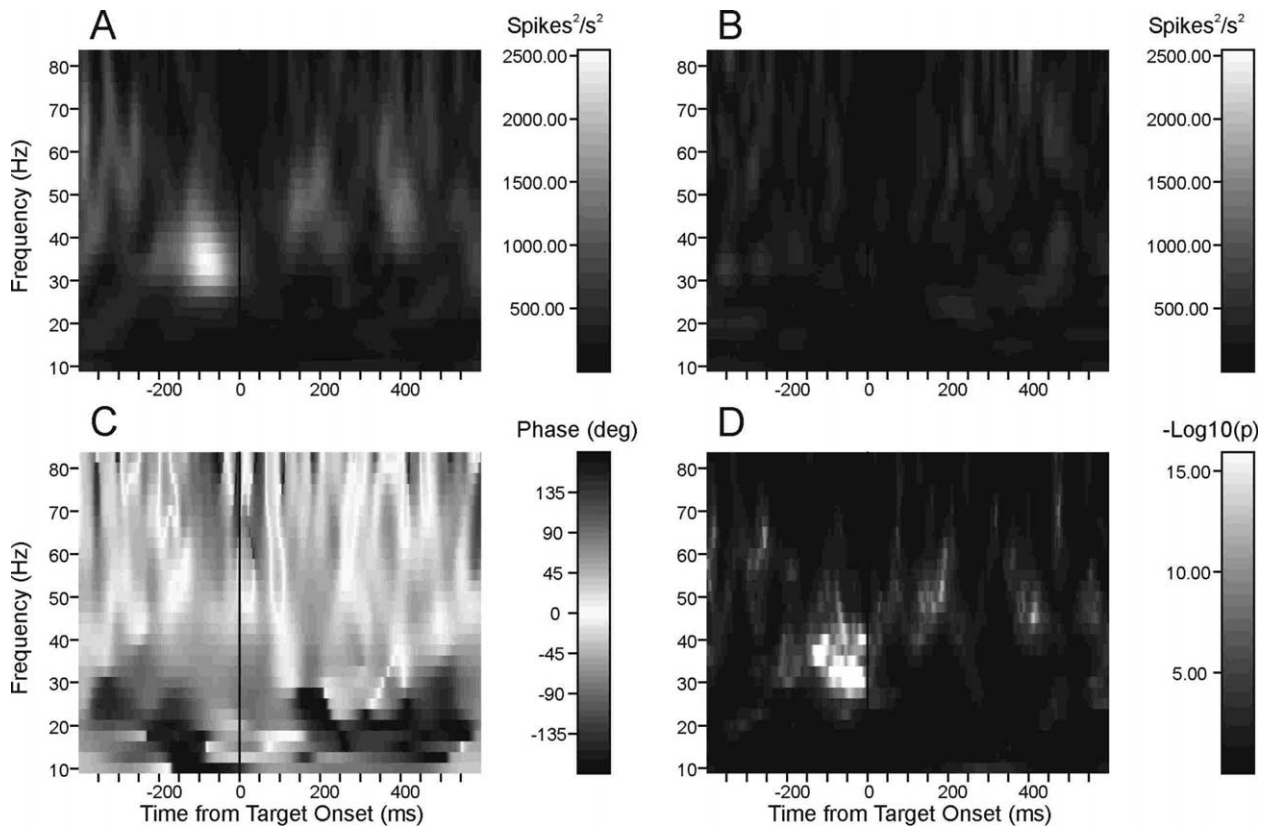


Fig. 3. Wavelet cross-spectrum of spike trains. (A) Amplitude of the wavelet cross-spectrum for the original spike trains (same as in Fig. 2). (B) Amplitude of the wavelet cross-spectrum for the shift predictor. (C) The phase of the wavelet cross-spectrum for the original spike trains. (D) The map of P -values for the wavelet cross-spectrum amplitude shown in A. This was calculated based on the normal probability density functions estimated from ten re-sampled wavelet cross-spectra (see Section 2).

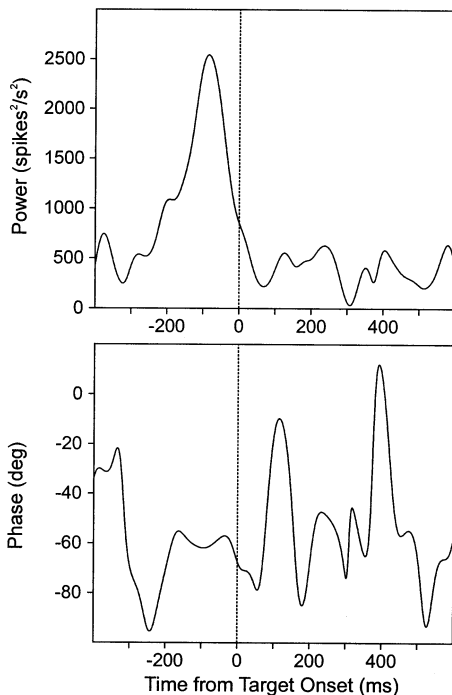


Fig. 4. The amplitude and the phase of the wavelet cross-spectrum shown in Fig. 3A for the frequency of 35 Hz.

distributional assumptions and therefore might provide more accurate evaluation of statistical significance, this procedure was too time-consuming to apply to a large number of neuron pairs. In the present analysis, the P -values calculated from 200-resampled wavelet cross-spectra provided a baseline to which the results of alternative methods were compared.

Second, a small number of re-sampled cross-spectra ($n = 10$) were used to estimate probability density functions for the original average cross-spectrum. In this method, it is important to apply an appropriate mathematical function to estimate the probability density function. The amplitude of the wavelet cross-spectrum often violated the normal distribution. According to the Kolmogorov–Smirnov test, the hypothesis that the wavelet cross-spectrum amplitude was normally distributed was rejected in 31.2% of all the time and frequency combinations examined in the present example. In contrast, square-root transforms successfully normalized the distribution of the amplitude. After square-root transformation, the null hypothesis was rejected in less than 3% of the time and frequency combinations, and this was less than the significance level used in the Kolmogorov–Smirnov test

($P = 0.05$). Based on these results, the square-root transformed amplitude of the wavelet cross-spectrum was assumed to be normally distributed, and the P -values were estimated from the normal probability density function with the mean and the S.D. obtained from ten re-sampled wavelet cross-spectra after square-root transformation. The resulting P -values, shown in Fig. 3D, were in good agreement with those of the permutation test ($r = 0.962$; Fig. 5). The RMS error between the P -values obtained from the normal probability density function and those of the permutation test was 0.08.

4. Discussion

Wavelet transforms have been applied to a variety of data in many different disciplines. In neurophysiology, wavelet transforms have been mostly adopted in the analysis of EEG data. In the present paper, these methods were applied to the multi-channel single-unit data, i.e. multiple spike trains recorded simultaneously. Whereas the EEG and local field potential recording data are analog signals sampled at regular intervals, spike trains are point processes defined solely by the arrival times of spikes. Despite such a fundamental difference in the nature of the signals, the present results indicate that the wavelet transforms can be successfully applied to a broad range of neurophysiological data, including spike trains.

There is a wide variety of methods based on the wavelet transforms that can be utilized in analyzing time series, such as spike trains (Percival and Walden, 2000).

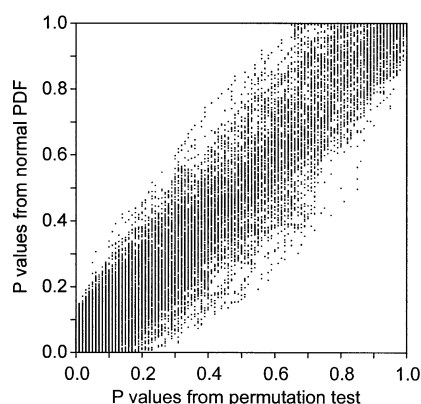


Fig. 5. Comparison of P -values from two different methods of evaluating the statistical significance of the wavelet cross-spectrum. The abscissa represents the P -values computed from a permutation test in which P -values were calculated using the empirical probability density functions estimated from 200 re-sampled wavelet cross-spectra. The ordinate represents P -values calculated using the normal probability density functions estimated from ten re-sampled wavelet cross-spectra (also shown in Fig. 3D).

In addition, these methods have advantages over more conventional methods based on Fourier transforms. For example, the Fourier power spectrum cannot handle non-stationary processes. The problem of non-stationarity can be addressed using short time Fourier transforms, but they suffer from the trade-off between temporal and spectral resolution due to the uncertainty principle (Papoulis, 1977). Wavelet transforms attempt to achieve an optimal solution to this problem by varying window size as a function of frequency. As pointed out in the previous application of wavelet transforms to the analysis of EEG data (Le Van Quyen et al., 2001; Quiroga and Schürmann, 1999; Sakowitz et al., 2001), such advantages of wavelet transforms are directly relevant to the analysis of spike train data, because spike trains are seldom stationary. In other words, it cannot be generally assumed that statistical properties of real spike trains remain invariant over time. To the contrary, these dynamic changes in the statistical properties of spike trains are usually the focus of investigations. For example, there is growing interest in the question of whether synchronization or phase-locked oscillation in neural activity has any functional significance. To obtain answers to this important question, methods based on wavelet transforms are likely to play an important role.

A method to evaluate statistical significance of the wavelet cross-spectrum has been previously proposed (Torrence and Compo, 1998). This method was based on the assumption that individual wavelet spectra follow χ^2 -distribution. In the present analysis, no systematic attempts were made to derive a theoretical probability density function, because it is likely that such distributions are affected by the statistical properties of the spike trains in question. In addition, the permutation test used in the present study required a large number of re-sampled cross-spectra, making it computationally demanding. A practical solution to this problem might be to estimate the probability density function for the amplitude of the wavelet cross-spectrum based on a smaller number of re-samples. In an initial trial of this approach, the use of ten re-samples produced results that were comparable to those obtained with the larger number of re-samples.

Although the wavelet cross-spectrum provides certain advantages over other methods, such as the TrCCF, its utility resides mostly in detecting temporally overlapping phase-locked oscillation in two parallel spike trains. In some cases, there may be a substantial delay between transient oscillatory discharges of different neurons. This form of temporally delayed phase-locked oscillation will not be detected by the wavelet cross-spectrum. In addition, different neurons might display oscillatory discharges in different frequency bands in a time-locked manner. Since the wavelet cross-spectrum examines the coherence in the oscillation that takes

places in each frequency separately, it will also fail to detect this type of temporal correlation. Methods based on bispectrum or bicoherence can be used to analyze temporal coupling between oscillatory discharges in different frequencies (Schanze and Eckhorn, 1997; von Stein et al., 2000). These methods are, however, based on the Fourier transform, and their utility in analyzing non-stationary spike trains is thereby limited. Therefore, without the methods that can fully characterize diverse patterns of temporal correlation, studies of multi-channel spike trains still remain a challenging task.

Acknowledgements

I thank Ryan P. Murray for his assistance in collecting the neural data, Dominic Barraclough for his suggestions on the manuscript and statistical analysis, and Joseph Malpeli and Rita Farrell for their help with the manuscript. This work was supported by the National Institute of Health Grants R01-MH59216 and P30-EY01319, and the McDonnell-Pew Cognitive Neuroscience Grant 99-27 from the James S. McDonnell Foundation.

References

- Aertsen AMHJ, Gerstein GL, Habib MK, Palm G. Dynamics of neuronal firing correlation: modulation of 'effective connectivity'. *J Neurophysiol* 1989;61:900–17.
- Baker SN, Spinks R, Jackson A, Lemon RN. Synchronization in monkey motor cortex during a precision grip task. I. Task-dependent modulation in single-unit synchrony. *J Neurophysiol* 2001;85:869–85.
- Bressler SL, Coppola R, Nakamura R. Episodic multiregional cortical coherence at multiple frequencies during visual task performance. *Nature* 1993;366:153–6.
- Csibra G, David G, Spratling MW, Johnson MH. Gamma oscillations and object processing in the infant brain. *Science* 2000;290:1582–5.
- Eckhorn R, Bauer R, Jordan W, Brosch M, Kruse W, Munk M, Reitboeck HH. Coherent oscillations—a mechanism of feature linking in the visual cortex—multiple electrode and correlation analyses in the cat. *Biol Cybern* 1988;60:121–30.
- Fries P, Roelfsema PR, Engel AK, Koenig P, Singer W. Synchronization of oscillatory responses in visual cortex correlates with perception in binocular rivalry. *Proc Natl Acad Sci USA* 1997;94:12699–704.
- Fries P, Reynolds JH, Rorie AE, Desimone R. Modulation of oscillatory neuronal synchronization by selective visual attention. *Science* 2001;291:1560–3.
- Gail A, Brinkmeyer HJ, Eckhorn R. Contour decouples gamma activity across texture representation in monkey striate cortex. *Cerebral Cortex* 2000;10:840–50.
- Gawne TJ, Richmond BJ. How independent are the messages carried by adjacent inferior temporal cortical neurons. *J Neurosci* 1993;13:2758–71.
- Gevins A, Smith ME, McEvoy L, Yu D. High-resolution EEG mapping of cortical activation related to working memory: effects of task difficulty, type of processing, and practice. *Cerebral Cortex* 1997;7:374–85.
- Gray CM. The temporal correlation hypothesis of visual feature integration: still alive and well. *Neuron* 1999;24:31–47.
- Gray CM, Singer W. Stimulus-specific neuronal oscillations in orientation columns of cat visual cortex. *Proc Natl Acad Sci USA* 1989;86:1698–702.
- Isoglu-Alkaç Ü, Basar-Eroglu C, Ademoglu A, Demiralp T, Miener M, Stadler M. Alpha activity decreases during the perception of Necker cube reversals: an application of wavelet transform. *Biol Cybern* 2000;82:313–20.
- Lee D, Port NL, Kruse W, Georgopoulos AP. Variability and correlated noise in the discharge of neurons in motor and parietal areas of the primate cortex. *J Neurosci* 1998;18:1161–70.
- Le Van Quyen M, Foucher J, Lachaux J-P, Rodriguez E, Lutz A, Martinerie J, Varela F. Comparison of Hilbert transform and wavelet methods for the analysis of neuronal synchrony. *J Neurosci Methods* 2001;111:83–98.
- MacPherson JM, Aldridge JWA. A quantitative method of computer analysis of spike train data collected from behaving animals. *Brain Res* 1979;175:183–7.
- Meyers SD, Kelly BG, O'Brien JJ. An introduction to wavelet analysis in oceanography and meteorology: with application to the dispersion of Yanai waves. *Mon Weather Rev* 1993;121:2858–66.
- Miltner WHR, Braun C, Arnold M, Witte H, Taub E. Coherence of gamma-band EEG activity as a basis for associative learning. *Nature* 1999;397:434–6.
- Mima T, Oluwatimilehin T, Hiraoka T, Hallett M. Transient inter-hemispheric neuronal synchrony correlates with object recognition. *J Neurosci* 2001;21:3942–8.
- Papoulis A. *Signal Analysis*. New York: McGraw-Hill, 1977.
- Papulis Q, Baker SN. An accurate measure of the instantaneous discharge probability, with application to unitary joint-event analysis. *Neural Comput* 2000;12:647–99.
- Percival DB, Walden AT. *Wavelet Methods for Time Series Analysis*. Cambridge: Cambridge University Press, 2000.
- Perkel DH, Gerstein GL, Moore GP. Neuronal spike trains and stochastic point processes. II. Simultaneous spike trains. *Biophys J* 1967;7:419–40.
- Portnoff MR. Time–frequency representations of digital signals and systems based on short time Fourier analysis. *IEEE Trans Acoust Speech Signal Process* 1980;28:55–69.
- Quiroga RQ, Schürmann M. Functions and sources of event-related EEG alpha oscillations studied with the wavelet transform. *Clin Neurophysiol* 1999;110:643–54.
- Rodriguez E, George N, Lachaux J-P, Martinerie J, Renault B, Varela F. Perception's shadow: long-distance synchronization of human brain activity. *Nature* 1999;397:430–3.
- Roelfsema PR, Engel AK, Konig P, Singer W. Visuomotor integration is associated with zero time-lag synchronization among cortical areas. *Nature* 1997;385:157–61.
- Sakowitz OW, Quiroga RQ, Schürmann M, Başar E. Bisensory stimulation increases gamma-responses over multiple cortical regions. *Cogn Brain Res* 2001;11:267–79.
- Sanes JN, Donoghue JP. Oscillations in local field potentials of the primate motor cortex during voluntary movement. *Proc Natl Acad Sci USA* 1993;90:4470–4.
- Sarnthein J, Petsche H, Rappelsberger P, Shaw GL, von Stein A. Synchronization between prefrontal and posterior association cortex during human working memory. *Proc Natl Acad Sci USA* 1998;95:7092–6.
- Schanze T, Eckhorn R. Phase correlation among rhythms present at different frequencies: spectral methods, application to microelectrode recordings from visual cortex and functional implications. *Int J Psychophysiol* 1997;26:171–89.
- Shadlen MN, Movshon JA. Synchrony unbound: a critical evaluation of the temporal binding hypothesis. *Neuron* 1999;24:67–77.

- Singer W. Neuronal synchrony: a versatile code for the definition of relations. *Neuron* 1999;24:49–65.
- Srinivasan R, Russell DP, Edelman GM, Tononi G. Increased synchronization of neuromagnetic responses during conscious perception. *J Neurosci* 1999;19:5435–48.
- Tallon-Baudry C, Bertrand O, Delpuech C, Pernier J. Oscillatory gamma-band (30–70 Hz) activity induced by a visual search task in humans. *J Neurosci* 1997;17:722–34.
- Tallon-Baudry C, Bertrand O, Peronnet F, Pernier J. Induced gamma-band activity during the delay of a visual short-term memory task in humans. *J Neurosci* 1998;18:4244–54.
- Tononi G, Srinivasan R, Russell DP, Edelman GM. Investigating neural correlates of conscious perception by frequency-tagged neuromagnetic responses. *Proc Natl Acad Sci USA* 1998;95:3198–203.
- Torrence C, Compo GP. A practical guide to wavelet analysis. *Bull Am Meteorol Soc* 1998;79:61–78.
- von Stein A, Rappelsberger P, Sarnthein J, Petsche H. Synchronization between temporal and parietal cortex during multimodal object processing in man. *Cerebral Cortex* 1999;9:137–50.
- von Stein A, Chiang C, Konig P. Top-down processing mediated by interareal synchronization. *Proc Natl Acad Sci USA* 2000;97:14748–53.
- Zohary E, Shadlen MN, Newsome WT. Correlated neuronal discharge rate and its implications for psychophysical performance. *Nature* 1994;370:140–3.